Available online at www.sciencedirect.com

ScienceDirect

journal homepage: http://www.elsevier.com/locate/euprot

Distribution analysis of the putative cancer marker S100A4 across invasive squamous cell carcinoma penile tissue

Brian Flatley[a,b], *Chris Quaye*[c], *Elizabeth Johnson*[c], *Alex Freeman*[d], *Asif Muneer*[e], *Suks Minhas*[e], *Jennifer C. Paterson*[f], *Fawaz Musa*[c], *Peter Malone*[b], *Rainer Cramer*[a,*]

[a] *Department of Chemistry, University of Reading, Reading, UK*
[b] *Urology Research Department, Royal Berkshire NHS Foundation Trust Hospital, Reading, UK*
[c] *Department of Cellular Pathology, Royal Berkshire NHS Foundation Trust Hospital, Reading, UK*
[d] *Department of Histopathology, University College London Hospital, London, UK*
[e] *Department of Urology, University College London Hospital, London, UK*
[f] *UCL Advanced Diagnostics, University College London, London, UK*

ARTICLE INFO

Article history:
Received 21 November 2014
Received in revised form
30 January 2015
Accepted 5 February 2015
Available online 16 February 2015

Keywords:
MALDI MS imaging
Penile cancer
S100A4
Biomarker discovery

ABSTRACT

MS-based proteomic methods were utilised for the first time in the discovery of novel penile cancer biomarkers. MALDI MS imaging was used to obtain the in situ biomolecular MS profile of squamous cell carcinoma of the penis which was then compared to benign epithelial MS profiles. Spectra from cancerous and benign tissue areas were examined to identify MS peaks that best distinguished normal epithelial cells from invasive squamous epithelial cells, providing crucial evidence to suggest S100A4 to be differentially expressed. Verification by immunohistochemistry resulted in positive staining for S100A4 in a sub-population of invasive but not benign epithelial cells.

1. Introduction

Penile cancer is a rare cancer in developed countries with approximately 500 cases diagnosed each year in the UK [1]. There is an increased incidence of penile cancer in South America and Western Africa, which has been putatively explained by the socioeconomic conditions and restricted access to health care in these countries [2]. Squamous cell carcinoma (SCC) is the most common subtype of penile cancer accounting for ~95% of new cases each year [3]. Other malignant tumour types include adenocarcinoma, lymphoma, melanoma, and various mesenchymal tumours such as Kaposi's sarcoma and leiomyosarcoma [4]. Premalignant conditions eponymously termed Bowen's disease, Erythroplasia de Queyrat and Bowenoid papulosis represent carcinoma in situ or penile intra-epithelial neoplasia (PeIN 3). These can develop into invasive SCC if left untreated [2]. The primary

* *Corresponding author at*: Department of Chemistry, University of Reading, Whiteknights, Reading RG6 6AD, UK. Tel.: +44 1183784550.
E-mail address: r.k.cramer@reading.ac.uk (R. Cramer).

http://dx.doi.org/10.1016/j.euprot.2015.02.001

treatment for penile cancer has moved to more conservative penile preserving techniques in order to maintain function. These include glansectomy and reconstruction and glans resurfacing procedures which have a good cosmetic and functional outcome compared to radical surgery. [5]. The lymphatic dissemination of penile cancer occurs in a predictable step-wise fashion; firstly to the inguinal nodes and subsequently to the pelvic nodes and then the para-aortic nodes [6]. Clinically the best prognostic indicator is the presence of metastatic inguinal lymph nodes [7]. However, despite a number of potential molecular biomarkers and the development of nomograms, there is as yet no reproducible biomarker available which is a reliable indicator for prognosis and metastatic potential in the primary tumour [8].

In the 1990s, matrix-assisted laser desorption/ionisation (MALDI) mass spectrometry imaging (MSI) was established [9,10]. MALDI MSI can be employed for the simultaneous in situ visualisation and spatial mapping of various classes of molecules, from drug metabolites [11] to large proteins [12,13]. The ability to detect signals in their native environment gives information on local production of biomolecules as well as their distribution across different disease states of the tissue. This information can be lost if a large-scale tissue digestion protocol is followed, such as in the more traditional bottom-up proteomics approach.

MALDI MSI provides an excellent platform upon which molecular pathology can be applied, giving the investigator a "first-view" of the global biomolecular profile of the tissue and the various micro-environments present [14]. It has successfully been applied to a number of cancers [15,16] to provide the basis for more targeted analysis either via the traditional immunohistochemistry route or more sophisticated shotgun-type mass spectrometry methods. In this study, we present MALDI MSI results showing differentially expressed biomolecules in penile cancer tissue. This initial primer experiment served as an excellent starting point to study the malignancy in its anatomical context. Furthermore, the immunoactivity of S100A4 protein in penile cancer tumour tissue was measured and its correlation to the clinical grading of the tumour was determined. From these measurements, it can be concluded that a sub-population of S100A4-positive epithelial cells exists in the tumour environment and is virtually absent in matched benign tissue.

2. Materials and methods

2.1. *Sample collection*

Fresh tissue specimens, superfluous to that required for diagnostic evaluation, were collected from patients undergoing surgery for the removal or biopsy of penile cancer at the Department of Urology, Royal Berkshire Hospital, Reading, UK. Formalin-fixed paraffin-embedded (FFPE) penile tissue was collected for immunohistochemistry at the Department of Urology, University College London Hospital, London, UK. All specimens were procured with the approval from the University of Reading and Berkshire Research Ethics committees (10/H0505/16) and full informed consent was granted by the participants.

2.2. *Tissue preparation and matrix application for MALDI MSI*

Two consecutive tissue slices with a thickness of 10 μm and 5 μm were cut from two different frozen tissue blocks (T1 and T2) from two different patients and labelled T1-10, T1-5, T2-10 and T2-5. The area of the T1-10 was approx. 16.5 mm × 15 mm and for T2-10 this was approx. 16.5 mm × 9.5 mm. A Leica CM3050 S cryostat microtome (Leica Biosystems, Peterborough, UK) was used to cut the slices from the fresh frozen tissue blocks, which were then thaw-mounted on ground steel MALDI target plates (Bruker Daltonics, Bremen, Germany) at −20 °C. The tissue slices were brought to room temperature under vacuum for 30 min. Tissue fixation and removal of salts and excess haemoglobin were done through a series of ethanol/water wash steps as described by Schwartz et al. [17]. Subsequently, the tissue slices were dried under vacuum for another 10 min. A matrix solution with a concentration of 10 mg/ml was made of sinapinic acid (Sigma–Aldrich Co. Ltd., Gillingham, UK) dissolved in a 60:39.8:0.2 solution of acetonitrile:water:trifluoroacetic acid, which were all MALDI grade reagents from Sigma–Aldrich. The tissue slices were spray-coated with the matrix solution using a TLC sprayer (Sigma–Aldrich) at an optimised distance of 30 cm. At this distance it was found that a light matrix coat was applied evenly and reproducibly across the slices. After spraying the tissue, it was allowed to dry for 5 min, before repeating the cycle. This process was repeated five times ensuring an even deposition of matrix was observed across the slice. A calibration spot consisting of a standard solution of proteins and peptides (Bruker Daltonics) was added beside the mounted tissue slice for calibration purposes.

2.3. *MS analysis and data processing*

Mass spectra were acquired over an *m/z* range of 2,000–18,000 in positive linear mode and a laser repetition rate of 50 Hz using an Ultraflex MALDI axial-TOF mass spectrometer (Bruker Daltonics) with the acquisition software FlexControl 3.0. Custom geometry files were created to specify the imaging area using the in-house software PIMSS [18]. Using AutoExecute in FlexControl, MS images were recorded with a 200-μm spatial resolution, averaging the data from 50 shots per image pixel. PIMSS was used to convert raw data files into Analyze 7.5 format for image visualisation in BioMap (Novartis, Basel, Switzerland; http://www.maldi-msi.org).

For further data analysis, a representative population of spectra from areas of different tissue pathology (70 spectra from each region of interest) were extracted from the data set of the T1-10 tissue slice. On these spectra, classification and statistical evaluation was performed using ClinProTools 2.1 (Bruker Daltonics). The spectra were first processed and peaks were detected using a signal-to-noise cut-off of 5. The peak intensity values used for subsequent analysis were based on peak height. A Mann–Whitney *U* test was used for pair-wise comparison of peak intensities from normal and cancerous regions.

2.4. H&E and S100A4 immunohistochemistry staining

2.4.1. Haematoxylin and eosin staining

A 5-μm-thick consecutive tissue slice of a slice that was used for MSI was mounted on a glass slide, immersed in neutral buffered formalin for 45 s and rinsed under running tap water. It was then put into a Harris haematoxylin solution for 1 min, followed by a second rinse under running water. The slice was briefly dipped into 0.5% acidic alcohol for 15 s, rinsed under running tap water and then placed in the bluing reagent sodium bicarbonate for 15 s. To complete the staining the slice was counterstained in Eosin Yellowish for 30 s and taken through increasing concentrations of alcohol (75/90/100%) before being immersed in the clearing agent Xylene (Genta Medical, Tockwith, UK). The stained and fixed slice had a coverslip placed over it using the mounting medium Pertex (Leica Biosystems, Newcastle Upon Tyne, UK).

2.4.2. Antibody optimisation and immunohistochemistry

The rabbit polyclonal anti-S100A4 antibody (A5114; Dako, Ely, UK) was chosen for use in this study due to its reported high specificity for S100A4 and suitability for use with formalin-fixed paraffin-embedded (FFPE) tissues. Several 3-μm-thick sections of an in-house research tissue microarray (TMA) block containing a variety of normal and neoplastic tissues were used for antibody optimisation on the Bond-III automated staining platform (Leica Biosystems, Newcastle Upon Tyne, UK). The sections underwent automated dewaxing, and endogenous peroxidase was blocked using 3–4% (v/v) hydrogen peroxide. The antibody was tested with a range of citrate-based (pH 6.0) and EDTA-based (pH 9.0) heat-induced epitope retrieval methods. Dilution curves for anti-S100A4 were carried out (1/100, 1/200, 1/500, 1/1000, 1/1500, 1/2000 and 1/3000) with 15 min incubation at ambient temperature. The signal was visualised using the Bond Polymer Refine Detection kit (DS9800) with DAB Enhancer (AR9432) and haematoxylin counterstain. The sections were reviewed and optimal conditions chosen based upon the criterion of background-free selective cellular labelling. The antibody was taken forward for use on 20 penile cancer cases at a dilution of 1/1000 with heat-induced epitope retrieval using a citrate-based (pH 6.0) retrieval solution for 20 min.

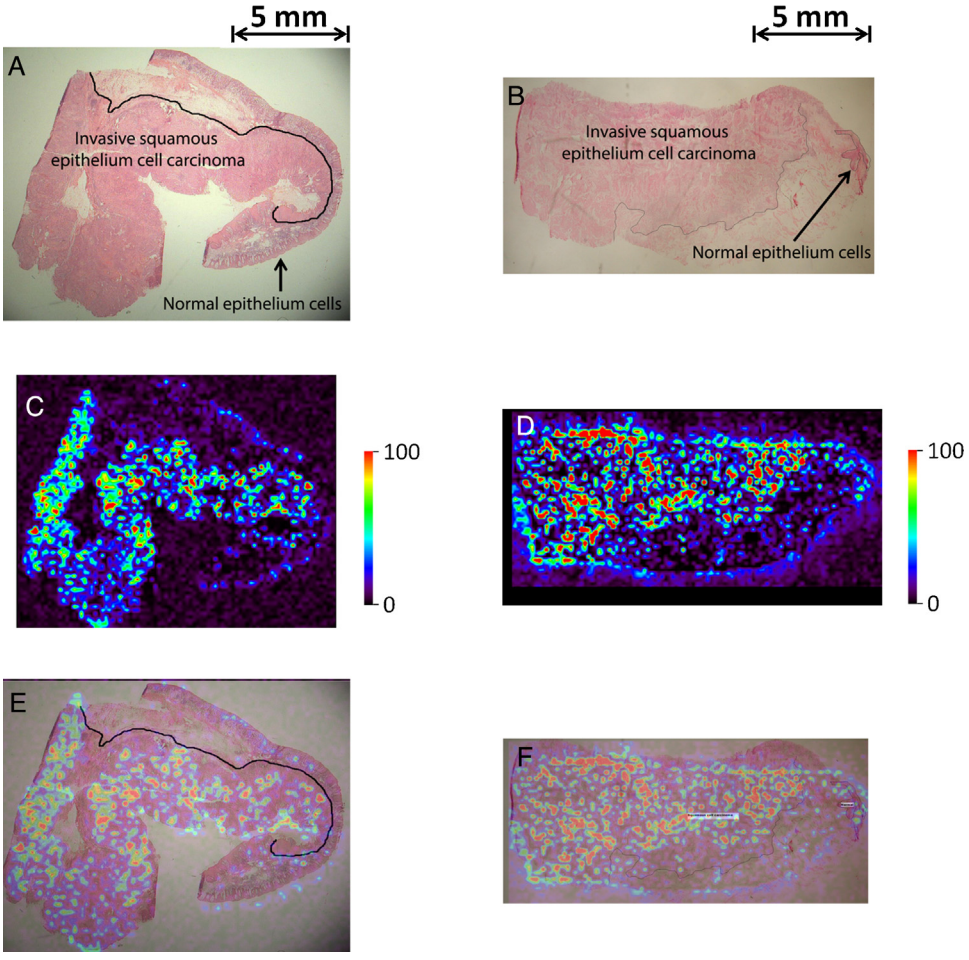

Fig. 1 – (A) and (B) show the H&E-stained T1-5 and T2-5 penile tissue slices with the regions of interest marked as identified by the histopathologist. The distribution of the *m/z* 11,637 ion across both the T1-10 and T2-10 slices, as obtained from the MSI data set, is given in (C) and (D). Panels (E) and (F) show an overlay of the highest signal intensity from the MSI images on top of the H&E images.

2.4.3. *Histopathological evaluation and analysis of S100A4 tissue staining*

All immunostained sections were examined by the same histopathologist using light microscopy. The clinical grading or diagnostic information for each case was not revealed to the histopathologist prior to this examination. The staining pattern of the S100A4-positive epithelial cells in the invasive tumour area was compared with that of the normal epithelial area in the same section. The staining within the invasive tumour areas was further examined by counting the number of positive-stained epithelial cells using high-power field (HPF) view (400× magnification) and taking care to avoid counting dendritic cells which also stained positive for S100A4. The area with the maximum number of S100A4-positive epithelial cells was thus located using low magnification and scanning the invasive region to identify the area where the highest number of positive cells was located. The staining pattern was classified as follows: five or less S100A4-positive cells in one HPF view as slightly positive (+), between six and nineteen S100A4-positive cells in one HPF view as positive (++), and finally twenty or more S100A4-positive epithelium cells in one HPF view as markedly positive (+++) [19]. A Chi square test was used to assess the correlation between the number of positive cells and the clinical grading of the cancer. For all statistical tests the level of significance was set at 0.05. One of the stained tissue slices, which only had carcinoma in situ was excluded from further evaluation.

3. Results

The 10 μm slices T1-10 and T2-10 were analysed by MALDI MSI, creating ion distribution maps with a lateral resolution of 200 μm, whilst the 5-μm-thick slices T1-5 and T2-5 were stained using a traditional haematoxylin and eosin (H&E) stain. The H&E staining patterns were examined by a histopathologist using light microscopy, and regions of benign and malignant squamous cell epithelium were marked on both T1-5 and T2-5 (see Fig. 1(A) and (B)). The tumour grade in both T1 and T2 was identified as Grade 2 (moderately differentiated) squamous cell carcinoma.

In T1-5, the histopathologist marked three distinct regions – invasive squamous epithelial cell carcinoma, Lichen Sclerosus (BXO) and hyperplastic epithelial cells (normal). Based on this report, regions of interest representing normal and cancerous areas were selected and spectra from both of these regions of T1-10 were exported to the ClinProTools software for peak identification and statistical analysis. After initial processing (baseline subtraction and smoothing) and normalisation against each slice's total ion current (TIC) value, a total of 107 individual peaks were identified across the two regions. Fig. 2 illustrates the average spectra from the cancer (A) and normal (B) region as obtained from ClinProTools analysis. The average intensity of each peak in the normal region and the cancerous region was compared using the Mann–Whitney *U* test (also known as Wilcoxon rank-sum test). Table 1 details the 10 most significantly different peaks between the two regions. The peak intensity at *m/z* 11,637 ± 2 was found to be significantly higher in the cancerous region of the tissue slice ($p < 0.05$). Using the software BioMap, the distribution of

Table 1 – List of the 10 most significantly different masses as measured using their MS signal intensities between the normal region and the cancerous region of tissue T1-10. The peaks are listed in decreasing order of statistical significance.

Peak number	*m/z*	*p*-Value of the Wilcoxon rank-sum test	Average peak intensity from normal tissue area	Standard deviation of intensity from normal tissue area	Average peak intensity from malignant tissue area	Standard deviation of intensity from malignant tissue area	Delta average (malignant compared to normal)
1	11,636.59	<0.000001	2.04	0.81	4.77	1.99	2.73
2	11,593.79	<0.000001	1.65	0.59	3.21	1.02	1.56
3	4932.61	<0.000001	38.09	14.64	86.49	35.81	48.40
4	5139.04	<0.000001	4.67	1.41	7.76	2.37	3.09
5	3452.81	<0.000001	7.13	3.04	3.6	1.43	−3.53
6	6270.19	<0.000001	7.46	4.01	3.75	1.46	−3.71
7	6642.29	<0.000001	12.93	6.44	6.8	2.33	−6.13
8	4021.74	<0.000001	2.61	0.9	1.71	0.57	−0.9
9	6171.16	<0.000001	2.62	0.76	1.85	0.59	−0.77
10	4029.74	<0.000001	2.5	1.12	1.54	0.59	−0.96

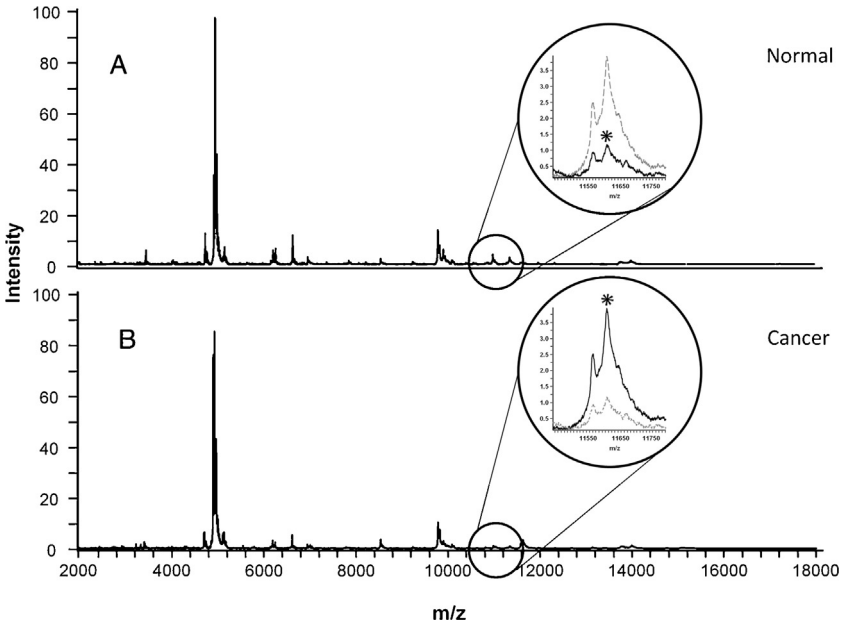

Fig. 2 – MALDI MS average spectra from normal (A) and cancer (B) epithelial cell regions of the T1-10 slice from tissue block T1. The spectra were all processed as described in Section 2, and the signal intensities at each *m/z* were compared to identify significant difference between the two regions. The most significantly different peak at *m/z* 11,637 is marked in both spectra with an asterisk.

the *m/z* 11,637 ion across the tissue in both T1-10 and T2-10 was visualised. The images in Fig. 1(C) and (D) show the signal intensity distribution of this ion and the images in Fig. 1(E) and (F) give an overlay of its signal intensity onto the H&E-stained slices. Supplementary Fig. 1 shows the distribution of *m/z* 4964 across the entire tissue section, showing that for some *m/z* the ion distribution was spread across both malignant and benign tissue sections whilst being confined to the tissue section only.

Supplementary Fig. 1 related to this article can be found, in the online version, at doi:10.1016/j.euprot.2015.02.001.

A peak at *m/z* 11,639 ± 2 was previously identified in the literature as S100 calcium-binding protein A4 (S100A4) [20]. The molecular weight of S100A4 in the UniProt human database is 11,729 Da. Taking into consideration that S100A4 loses its N-terminal methionine (-131 Da) upon activation and is also known to undergo acetylation (+42 Da), the expected *m/z* value of the singly charged S100A4 would be 11,641. The decision was taken to further investigate the potential association of S100A4 in penile carcinoma as it was found to have the most significant signal difference across the tissue sections. The identity of other biomolecular entities in Table 1 was investigated in a similar way as that for S100A4. The peak at *m/z* 4932.6 could be putatively identified as Thymosin Beta 10 [21], a protein that has previously been found to be over-expressed in a number of cancers including thyroid and hepatocellular carcinoma [22,23]. To identify the underlying biomolecular entity for the remainder of the peaks in Table 1, one would need to undertake a more detailed on-tissue bottom-up proteomics approach.

Thus, 20 tissue slices from formalin-fixed paraffin-embedded (FFPE) penile tissue blocks were immunostained with an S100A4 antibody. The immunostaining showed that there was no expression of S100A4 in normal epithelial cells or areas of lichen sclerosis. However, in the proliferating tumour regions small sub-populations of S100A4-positive cells were detected. In order to assess only epithelial cells, care had to be taken within the tumour region to distinguish between epithelial and dendritic cells, as the S100A4 antibody labelled both cell types (see Fig. 3). Dendritic cells differ from epithelial cells in morphology, possessing long cytoplasmic arms (dendrites) that extend from the nucleus, whereas epithelium cells are typically rounder. Where there was any uncertainty in the cell type, the cell in question was not counted as a positive cell. Table 2 details the results from the positive cell counting immunostaining experiment with the S100A4 antibody. A significant correlation was found ($p = 0.017$) using a Chi square test between the increasing number of positive S100A4 cells

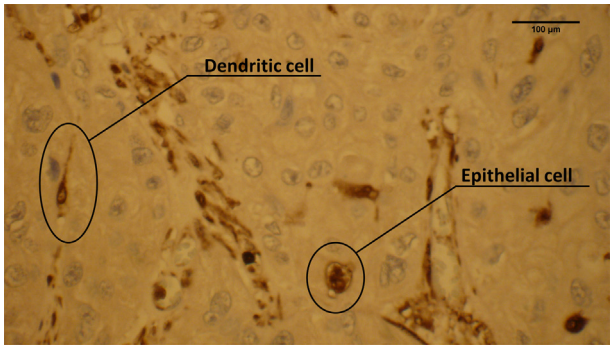

Fig. 3 – A high power field (HPF) view (400×) of an area of S100A4 antibody-stained tissue with both positive dendritic and epithelial cells marked. The different morphological features of the two cell types are clearly visible (see text for details).

Table 2 – Results of the S100A4 immunohistochemical of the penile cancer specimens along with metadata for each sample.

Sample number	No. of positive S100A4 cells	Pathology grade	Stage[a]	Lymph node[a]
1	3	1	PT1	N0
2	4	2	PT2	N0
3	5	3	PT3	N0
4	6	2	PT1	N0
5	7	2	PT1	N0
6	11	2	PT1	N0
7	11	2	PT2	N2
8	11	2	PT2	N0
9	17	3	PT2	N0
10	20	2	PT1	N0
11	20	2	PT2	N0
12	20	3	PT1	N0
13	20	3	PT2	N0
14	20	3	PT2	N2
15	20	3	PT2	N0
16	20	3	PT2	N0
17	20	3	PT3	N2
18	20	3	PT3	N3
19	20	3	PT3	N0
20[b]	17			

[a] PT1–PT3 represent the primary tumour stages whilst N0–N3 represent the nodal tumour stages, using the TNM staging system.
[b] This sample is the lymph node tissue from sample no. 17.

counted in the invasive region of the tissue and the clinical grade of the removed tumour (as taken from the pathology report). Fig. 4 shows that 80% of the pathology Grade 3 tumours were markedly positive for S100A4. Only two out of the 10 Grade 3 tumours were found to have less than 20 positive cells per HPF. Although there was only one Grade 1 tumour in the sample cohort, it was only slightly positive for S100A4. Importantly, the results show that the majority of the Grade

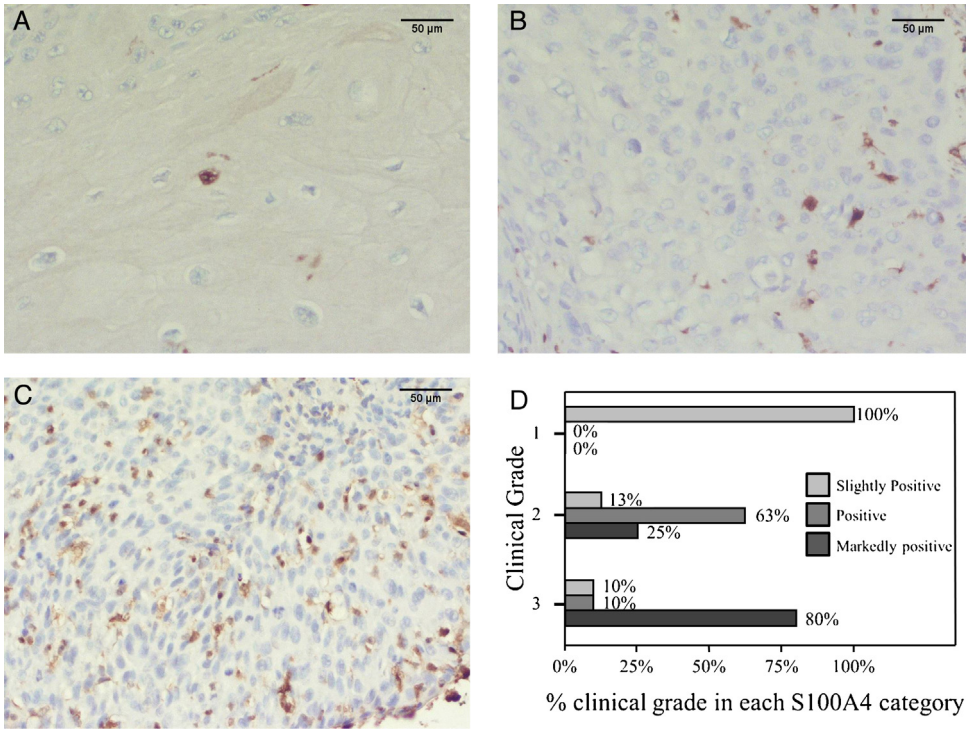

Fig. 4 – S100A4 expression in invasive penile squamous cell carcinoma. (A) Slightly positive (+) S100A4 immunoactivity with five or less S100A4-positive epithelial cells. (B) Positive (++) S100A4 immunoactivity with between six and nineteen S100A4-positive epithelial cells. (C) Markedly positive (+++) S100A4 immunoactivity with twenty or more S100A4-positive epithelial cells. All images were taken at 200× magnification. The graph in (D) shows the percentage of each clinical grade in the three categories for S100A4 positive staining.

2 tumours could be separated from the Grade 3 tumours by examining the immunoreactivity of S100A4 in the invasive regions (Fig. 4(D)).

For one of the participants both a primary tumour and a metastatic lymph node sample were provided. In this case, S100A4-positive epithelial cells were also observed to be present in the invasive islands of the lymph node metastasis in addition to those found in the primary tumour.

4. Discussion

MSI experiments can generate data files well in excess of 1 Gb per image depending on the mass range, pixel size and image size. This data set enables the user to view the distribution of any ions measured across the tissue surface. Advantages of MSI experiments include the small amount of sample that is consumed in a single analysis and the ability to directly compare the ion distribution map with histology results from a consecutive tissue slice [24]. MALDI MSI experiments have proven very successful at identification of potential biomarkers, even when small cohorts are used in the initial experiments. In this case study we directly compared ion distribution maps created from two separate penile tissue blocks removed during surgery for penile carcinoma with consecutive H&E-stained slices to investigate the localisation of specific ion signals in areas of different pathology, i.e. tumour regions versus regions of similar cellular origin that show no sign of malignancy (benign/normal epithelial cells).

Due to the large number of data points that were collected during the imaging experiments, it would have been labour- and time-consuming, along with an increased risk of missing significant results, to scroll through each ion distribution map and evaluate if there was differential expression in specific regions of the tissue. By taking the representative spectra from sufficiently large areas of the tumour and normal region, constructing an averaged peak list and subjecting it to comparative analysis it allowed the identification of ion signals that were significantly different between the different pathological regions of the tissue. As the data of Fig. 1(E) and (F) show, the distribution of the ion signal at m/z 11,637 is confined to the invasive epithelial cellular regions, whereas at other m/z ratios the ion signal distribution is spread equally across the entire epithelial cellular region of the tissue slice.

Although we were unable to identify the biomolecule responsible for this difference in signal intensity by mass spectrometry, despite trying on-tissue enzymatic digestion [25] and laser-capture microdissection methods [26,27], the published literature suggests that this peak can be attributed to the protein S100A4. Stoeckli et al. reported in 2001 that they identified a peak at m/z $11{,}639 \pm 3$ as S100A4 with an increased signal intensity in glioblastoma tumour regions from MSI experiments [20]. This result is also recorded in both bottom-up and top-down experiments in the MaTisse database [28]. Further support for this assignment was found in the UniProt human database sequence entry, indicating that the activated form of S100A4 could indeed be the underlying protein.

Similar to previously published research in various cancers, e.g. ovarian [16], colon [15], and gastric cancer [29], MALDI MSI was used to effectively monitor hundreds of compounds across the tissue surface in a case-study cohort, and statistical analysis enables the initial first-pass identification of the more discriminating peaks between normal and malignant environments. Based on the identification information a study population of penile tumour tissue slices was investigated by an immunoassay using an S100A4-specific antibody. Evaluation of the immunoassay results found that despite the small sample size there was a significant correlation between the number of S100A4 positive epithelial cells in the invasive tumour and the histopathological grade of the cancer ($p = 0.017$).

S100 calcium-binding proteins are small, acidic proteins (10–12 kDa) and are part of the larger Ca^{2+}-binding EF-hand motif superfamily [30]. They have a broad range of intra- and extracellular functions including regulation of protein phosphorylation and the modulation of the cytoskeleton dynamics in metastatic cells [31], and are also involved in calcium homeostasis and the regulation of transcription factors [32]. It is known that the over-expression of S100A4 in cells can cause disruption of p53 phosphorylation [30,33], which can lead to a decrease in apoptosis and an increase in cell proliferation and tumour growth. The role of p53 as a possible prognostic marker, along with its general role in HPV-dependent penile cancer progression, has been investigated in previously published research [34]. It was found by Martins et al. that the over-expression of p53 was associated with tumour progression and the cause of specific cell death [34].

So far only a few penile cancer-specific candidate markers have been described. For instance, Campos et al. investigated E-cadherin levels in penile cancer and found a significant correlation between lower expression levels of E-cadherin and an increased risk of lymph node metastasis [35]. E-cadherin is one of the most important molecules in cell–cell adhesion in epithelial tissue, and a decrease in its expression is linked with metastatic cells that grow and function without the normal regulated cellular environment [36]. Interestingly, increased levels of S100A4 have previously been reported to be concomitant with reduced levels of E-cadherin in many different tumours including non-small cell lung cancer [37], malignant melanoma [38] and oral squamous cell carcinoma [39]. Campos et al. also investigated the matrix metalloproteinases MMP-2 and MMP-9 and evaluated their potential as prognostic markers for lymph node metastasis from penile cancer. Matrix metalloproteinase proteins are a group of zinc enzymes that are responsible for degradation of extracellular matrix components such as collagens and proteoglycans [40]. Campos et al. found that neither showed any correlation with an increased risk of lymph node metastasis, but that the level of MMP-9 was an independent risk factor for disease recurrence [35]. These observations are important indicators of the role that S100A4 plays in the biological progress of penile cancer. The reduction of adhesion as indicated by the loss of E-cadherin is one marker for cells undergoing epithelial–mesenchymal transition (EMT), and S100A4 is known to be a master mediator in EMT [41], whilst S100A4's interaction with Annexin II and MMP proteins is thought to promote metastasis by inducing remodelling of the extracellular matrix and

as a result to facilitate angiogenesis and tumour invasion [42,43].

From the immunohistochemical results of the tissue sections using an S100A4-specific antibody, the tumour environment was shown to have a heterogeneous population of invading epithelial cells. The immunostaining results were semi-quantitatively measured and using the results of the statistical analysis a significant correlation between the number of S100A4-positive cells and the histopathological grade of the tumour. It has been widely hypothesised recently that this cellular diversity or heterogeneity within the tumour could be a result of small population of cancer stem cells or cancer-initiating cells (CICs) [44–47]. If, following further validation, the findings were found to hold true and the aggressiveness of the cancer along with the chances of detecting positive lymph nodes earlier could be tested through the immunoassay staining for presence of S100A4 protein, the assay could be translated to a more automated method of staining evaluation, e.g. CMYK.

In the pathologically related head and neck squamous cell carcinoma, a sub-population of S100A4-positive cells was observed by Lo et al. [19]. They found that the S100A4 pathway played a critical role in maintaining the stem-cell like properties of a sub-population of cells within the tumour that are proposed to be CICs or cancer stem cells. Another of their findings was that the increased signalling of S100A4 within this tumour increased the tumourigenicity of the cells in question [19]. Similar to this study they reported a significant correlation between S100A4 expression and the clinical grading of the head and neck cancer, and in addition found a correlation between patient survival and increased levels of the stemness markers Nanog and Oct-4. Given that these two squamous cell malignancies are pathologically so closely related it can be postulated that the expression of S100A4 in the sub-population of invasive cells in penile cancer plays a similarly critical role as in head and neck squamous cell carcinoma.

Prognosis for penile cancer following removal of the primary tumour depends on the lymph node status. If there are clinically impalpable inguinal lymph nodes (cN0) then the risk of harbouring occult metastases is approximately 20% [6]. Lymphadenectomy before the nodes become palpable infers a survival advantage but carries a significant morbidity risk and would mean overtreatment of 80% of patients. Although dynamic sentinel lymph node biopsy has addressed this in some centres worldwide, the false negative rate is still 7%. Better risk stratification could mean fewer lymphadenectomies for men that do not need them and earlier lymph node removal for those that do (i.e. prior to them becoming palpable), thus reducing morbidity and mortality. The results reported here show that increasing histopathological grades of penile cancer have higher numbers of S100A4-positive cells within the invasive islands. Taking into account that the trial cohort was quite small, the results need to be verified using a larger number of participants. To further improve the detection and evaluation of the staining patterns of S100A4 in malignant tissue, digital pathology could be used (methods such as CMYK). The early promise shown by S100A4 certainly justifies further investigation into its prognostic use.

5. Conclusion

MALDI MSI afforded the detection of tumour-associated ions in the invasive areas of penile cancer tissue slices, demonstrating the potential of the MSI technique to uncover novel tumour-specific markers for penile cancer. The significant difference in the peak signal intensity at *m/z* 11,637 between the averaged normal and cancer spectra taken from sufficiently large tissue regions was also reflected in the ion distribution image for this particular *m/z* value. Using literature and known protein sequence data, the peak was putatively assigned to the protein S100A4. S100A4 protein levels were also measured in a larger sample population by immunohistochemistry and it was found that there was a significant correlation between the number of positive cells in the tissue and the clinical tumour-grading. However, to further clarify the prognostic (staging) power of S100A4 in squamous cell carcinoma of the penis, additional studies with a larger number of cancer specimens as well as follow-up studies on survival rates are needed. A second strand of follow-up analysis will be to investigate the remaining peaks from Table 1 (including Thymosin Beta 10) and carry out both an initial immunohistochemistry analysis to evaluate the biomarker and then to progress both S100A4 and of the other peaks to large-scale clinical validation.

Examining S100A4-specific staining in the primary tumour of patients with penile cancer may offer complementary information that could aid the pathologist in assessing the aggressiveness of the cancer and increase the chances of detecting positive lymph nodes earlier and/or without the need for further biopsies.

Significance

Our study demonstrates the application of mass spectrometry imaging for the identification of molecular species capable of distinguishing between benign and malignant penile tissue. In a follow-on study S100A4 was shown to be heterogeneously distributed in malignant penile tissue. This case study is very significant as research into penile cancer is rare and an initial study such as the one presented in this manuscript offers exciting new insights into potential cell differentiation across malignant tissue in penile cancer.

Conflict of interest

The authors have no relevant financial or other beneficial interests to disclose.

Transparency document

The Transparency document associated with this article can be found in the online version.

Acknowledgments

This research was supported through a PhD studentship grant by the Royal Berkshire Hospital NHS Trust. We thank the

Chemical Analysis Facility at the University of Reading for access to the Ultraflex mass spectrometer.

REFERENCES

[1] CancerStats report – Penile Cancer UK. Cancer Research UK; 2011.
[2] Salvioni R, Necchi A, Piva L, Colecchia M, Nicolai N. Penile cancer. Urol Oncol 2009;27:677–85.
[3] Mistry T, Jones RW, Dannatt E, Prasad KK, Stockdale AD. A 10-year retrospective audit of penile cancer management in the UK. BJU Int 2007;100:1277–81.
[4] Kayes O, Ahmed HU, Arya M, Minhas S. Molecular and genetic pathways in penile cancer. Lancet Oncol 2007;8:420–9.
[5] Minhas S, Kayes O, Hegarty P, Kumar P, Freeman A, Ralph D. What surgical resection margins are required to achieve oncological control in men with primary penile cancer. BJU Int 2005;96:1040–3.
[6] Pizzocaro G, Algaba F, Horenblas S, Solsona E, Tana S, Van Der Poel H, et al. EAU penile cancer guidelines 2009. Eur Urol 2009;57:1002–12.
[7] Protzel C, Alcaraz A, Horenblas S, Pizzocaro G, Zlotta A, Hakenberg OW. Lymphadenectomy in the surgical management of penile cancer. Eur Urol 2009;55:1075–88.
[8] Muneer A, Kayes O, Ahmed HU, Arya M, Minhas S. Molecular prognostic factors in penile cancer. World J Urol 2009;27:161–7.
[9] Spengler B, Hubert M, Kaufmann R. MALDI ion imaging and biological ion imaging with new scanning UV-laser microprobe (P1041). In: 42nd ASMS conference on mass spectrometry. 1994.
[10] Caprioli RM, Farmer TB, Gile J. Molecular imaging of biological samples: localization of peptides and proteins using MALDI-TOF MS. Anal Chem 1997;69:4751–60.
[11] Cornett DS, Frappier SL, Caprioli RM. MALDI-FTICR imaging mass spectrometry of drugs and metabolites in tissue. Anal Chem 2008;80:5648–53.
[12] van Remoortere A, van Zeijl RJM, van den Oever N, Franck J, Longuespée R, Wisztorski M, et al. MALDI imaging and profiling MS of higher mass proteins from tissue. J Am Soc Mass Spectrom 2010;21:1922–9.
[13] Franck J, Longuespee R, Wisztorski M, Van Remoortere A, Van Zeijl R, Deelder A, et al. MALDI mass spectrometry imaging of proteins exceeding 30,000 daltons. Med Sci Monit 2010;16:BR293–9.
[14] Longuespee R, Fleron M, Pottier C, Quesada-Calvo F, Meuwis MA, Baiwir D, et al. Tissue proteomics for the next decade? Towards a molecular dimension in histology. Omics 2014;18:539–52.
[15] Meding S, Balluff B, Elsner M, Schone C, Rauser S, Nitsche U, et al. Tissue-based proteomics reveals FXYD3, S100A11 and GSTM3 as novel markers for regional lymph node metastasis in colon cancer. J Pathol 2012;4:459–70.
[16] Longuespee R, Gagnon H, Boyon C, Strupat K, Dauly C, Kerdraon O, et al. Proteomic analyses of serous and endometrioid epithelial ovarian cancers – cases studies – molecular insights of a possible histological etiology of serous ovarian cancer. Proteomics Clin Appl 2013;7:337–54.
[17] Schwartz SA, Reyzer ML, Caprioli RM. Direct tissue analysis using matrix-assisted laser desorption/ionization mass spectrometry: practical aspects of sample preparation. J Mass Spectrom 2003;38:699–708.
[18] Sarsby J, Towers MW, Stain C, Cramer R, Koroleva OA. Mass spectrometry imaging of glucosinolates in *Arabidopsis* flowers and siliques. Phytochemistry 2012;77:110–8.
[19] Lo JF, Yu CC, Chiou SH, Huang CY, Jan CI, Lin SC, et al. The epithelial–mesenchymal transition mediator S100A4 maintains cancer-initiating cells in head and neck cancers. Cancer Res 2011;71:1912–23.
[20] Stoeckli M, Chaurand P, Hallahan DE, Caprioli RM. Imaging mass spectrometry: a new technology for the analysis of protein expression in mammalian tissues. Nat Med 2001;7:493–6.
[21] Oppenheimer SR, Mi D, Sanders ME, Caprioli RM. Molecular analysis of tumor margins by MALDI mass spectrometry in renal carcinoma. J Proteome Res 2010;9:2182–90.
[22] Wang H, Jiang S, Zhang Y, Pan K, Xia J, Chen M. High expression of thymosin beta 10 predicts poor prognosis for hepatocellular carcinoma after hepatectomy. World J Surg Oncol 2014;12:226.
[23] Zhang XJ, Su YR, Liu D, Xu DB, Zeng MS, Chen WK. Thymosin beta 10 correlates with lymph node metastases of papillary thyroid carcinoma. J Surg Res 2014;192:487–93.
[24] Deininger SO, Ebert MP, Futterer A, Gerhard M, Rocken C. MALDI imaging combined with hierarchical clustering as a new tool for the interpretation of complex human cancers. J Proteome Res 2008;7:5230–6.
[25] Djidja MC, Claude E, Snel MF, Scriven P, Francese S, Carolan V, et al. MALDI-ion mobility separation-mass spectrometry imaging of glucose-regulated protein 78 kDa (Grp78) in human formalin-fixed, paraffin-embedded pancreatic adenocarcinoma tissue sections. J Proteome Res 2009;8:4876–84.
[26] Emmert-Buck MR, Bonner RF, Smith PD, Chuaqui RF, Zhuang Z, Goldstein SR, et al. Laser capture microdissection. Science 1996;274:998–1001.
[27] Espina V, Milia J, Wu G, Cowherd S, Liotta LA. Laser capture microdissection. Methods Mol Biol 2006;319:213–29.
[28] Maier SK, Hahne H, Gholami AM, Balluff B, Meding S, Schoene C, et al. Comprehensive identification of proteins from MALDI imaging. Mol Cell Proteomics 2013;12:2901–10.
[29] Balluff B, Rauser S, Meding S, Elsner M, Schone C, Feuchtinger A, et al. MALDI imaging identifies prognostic seven-protein signature of novel tissue markers in intestinal-type gastric cancer. Am J Pathol 2011;179:2720–9.
[30] Helfman DM, Kim EJ, Lukanidin E, Grigorian M. The metastasis associated protein S100A4: role in tumour progression and metastasis. Br J Cancer 2005;92:1955–8.
[31] Donato R. S100: a multigenic family of calcium-modulated proteins of the EF-hand type with intracellular and extracellular functional roles. Int J Biochem Cell Biol 2001;33:637–68.
[32] Salama I, Malone PS, Mihaimeed F, Jones JL. A review of the S100 proteins in cancer. Eur J Surg Oncol 2008;34:357–64.
[33] Grigorian M, Andresen S, Tulchinsky E, Kriajevska M, Carlberg C, Kruse C, et al. Tumor suppressor p53 protein is a new target for the metastasis-associated Mts1/S100A4 protein: functional consequences of their interaction. J Biol Chem 2001;276:22699–708.
[34] Martins AC, Faria SM, Cologna AJ, Suaid HJ, Tucci Jr S. Immunoexpression of p53 protein and proliferating cell nuclear antigen in penile carcinoma. J Urol 2002;167:89–92.
[35] Campos RS, Lopes A, Guimaraes GC, Carvalho AL, Soares FA. E-cadherin, MMP-2, and MMP-9 as prognostic markers in penile cancer: analysis of 125 patients. Urology 2006;67:797–802.
[36] Vleminckx K, Vakaet Jr L, Mareel M, Fiers W, van Roy F. Genetic manipulation of E-cadherin expression by epithelial tumor cells reveals an invasion suppressor role. Cell 1991;66:107–19.
[37] Kimura K, Endo Y, Yonemura Y, Heizmann CW, Schafer BW, Watanabe Y, et al. Clinical significance of S100A4 and

E-cadherin-related adhesion molecules in non-small cell lung cancer. Int J Oncol 2000;16:1125–31.
[38] Andersen K, Nesland JM, Holm R, Florenes VA, Fodstad O, Maelandsmo GM. Expression of S100A4 combined with reduced E-cadherin expression predicts patient outcome in malignant melanoma. Mod Pathol 2004;17:990–7.
[39] Moriyama-Kita M, Endo Y, Yonemura Y, Heizmann CW, Miyamori H, Sato H, et al. S100A4 regulates E-cadherin expression in oral squamous cell carcinoma. Cancer Lett 2005;230:211–8.
[40] Woessner JF. Matrix metalloproteinases and their inhibitors in connective-tissue remodeling. FASEB J 1991;5:2145–54.
[41] Stein U, Arlt F, Walther W, Smith J, Waldman T, Harris ED, et al. The metastasis-associated gene S100A4 is a novel target of beta-catenin/T-cell factor signaling in colon cancer. Gastroenterology 2006;131:1486–500.
[42] Garrett SC, Varney KM, Weber DJ, Bresnick AR. S100A4, a mediator of metastasis. J Biol Chem 2006;281:677–80.
[43] Semov A, Moreno MJ, Onichtchenko A, Abulrob A, Ball M, Ekiel I, et al. Metastasis-associated protein S100A4 induces angiogenesis through interaction with Annexin II and accelerated plasmin formation. J Biol Chem 2005;280:20833–41.
[44] Reya T, Morrison SJ, Clarke MF, Weissman IL. Stem cells, cancer, and cancer stem cells. Nature 2001;414:105–11.
[45] Prince ME, Sivanandan R, Kaczorowski A, Wolf GT, Kaplan MJ, Dalerba P, et al. Identification of a subpopulation of cells with cancer stem cell properties in head and neck squamous cell carcinoma. Proc Natl Acad Sci U S A 2007;104:973–8.
[46] Clarke MF, Becker MW. Stem cells: the real culprits in cancer. Sci Am 2006;295:52–9.
[47] Clarke MF, Dick JE, Dirks PB, Eaves CJ, Jamieson CH, Jones DL, et al. Cancer stem cells – perspectives on current status and future directions: AACR Workshop on cancer stem cells. Cancer Res 2006;66:9339–44.